Magnetoelectric and Magnetic Properties of Aluminum Borates $Ho_{1-x}Nd_xAl_3(BO_3)_4$

N. V. Volkov[a], I. A. Gudim[a], A. A. Demidov[b]*, and E. V. Eremin[a]

[a] Kirensky Institute of Physics, Siberian Branch, Russian Academy of Sciences, Krasnoyarsk, 660036 Russia
[b] Bryansk State Technical University, Bryansk, 241035 Russia
* e-mail: demandr@yandex.ru
Received December 17, 2014; in final form, December 23, 2014

The magnetoelectric and magnetic properties of substituted aluminum borates $Ho_{1-x}Nd_xAl_3(BO_3)_4$ have been studied experimentally and theoretically. A large magnetoelectric effect exceeding all known values in isostructural compounds except for $HoAl_3(BO_3)_4$ has been found. The magnetoelectric polarization of $Ho_{0.8}Nd_{0.2}Al_3(BO_3)_4$ and $Ho_{0.5}Nd_{0.5}Al_3(BO_3)_4$ at $T = 5$ K in a field of 9 T is $\Delta P_{ab}(B_b) \approx -2630$ and 1380 $\mu C/m^2$, respectively. A theoretical consideration based on the crystal field model for the rare-earth ion made it possible to interpret all measured properties within the unified approach. The crystal field parameters have been determined. The temperature (3−300 K) and field (up to 9 T) dependences of the magnetization and the temperature (5−100 K) and field (up to 9 T) dependences of the polarization have been described. The studied properties of $Ho_{1-x}Nd_xAl_3(BO_3)_4$ have been compared with those of $HoAl_3(BO_3)_4$ demonstrating record-high polarization values.

INTRODUCTION

Trigonal rare-earth borates $RM_3(BO_3)_4$ (M = Fe, Al, Cr, Ga, Sc) have been intensely studied in the last decade owing to their interesting physical properties and their variety at different combinations of R and M elements (see, e.g., [1−6] and review [7]). It was established that borates with two magnetic subsystems (iron borates $RFe_3(BO_3)_4$) belong to multiferroics [1, 3, 7]. It has been established recently that aluminum borates $RAl_3(BO_3)_4$ known for their nonlinear optical properties, which are borates with one magnetic subsystem, demonstrate colossal magnetoelectric polarization [6, 8−11]. In $HoAl_3(BO_3)_4$, the magnetoelectric polarization record-high for multiferroics at $T = 5$ K in a field of 9 T is $\Delta P_{ab}(B_b) \approx -5240$ $\mu C/m^2$ [11] and is several times higher than the known maximum polarization values, including those in iron borates.

It was shown in [12] that the difference in the polarization values in $HoFe_3(BO_3)_4$ and $HoAl_3(BO_3)_4$ is mainly due to the difference in the magnetostriction values. The anomalous temperature dependence of the polarization was found in $TbAl_3(BO_3)_4$. It is associated with the population of the upper energy levels of the ground multiplet of the Tb^{3+} ion increasing with the temperature [6]. However, no complete understanding of the mechanisms of the magnetoelectric interaction in aluminum borates and the role of the R ion in the occurring processes is achieved yet.

It is of high interest to synthesize and study new aluminum borates, e.g., substituted compounds $R^{(1)}_{1-x}R^{(2)}_xAl_3(BO_3)_4$ providing an even higher variety of observed effects and, probably, their enhancement. For example, it was revealed in [13] that the maximum polarization value in the substituted iron borate $Ho_{0.5}Nd_{0.5}Fe_3(BO_3)_4$ is higher than that in pure $HoFe_3(BO_3)_4$. It is reasonable to expect that the polarization in the aluminum borate $Ho_{1-x}Nd_xAl_3(BO_3)_4$ will be similarly increased as compared to the record-high ΔP value in $HoAl_3(BO_3)_4$. The use of Nd^{3+} ions in substituted aluminum borates is also promising, since one of the highest ΔP values in iron borates was found in $NdFe_3(BO_3)_4$. No information about the measurements of $\Delta P(B)$ in pure $NdAl_3(BO_3)_4$ is available in the literature.

This study is aimed at the synthesis and the experimental and theoretical study of the magnetoelectric and magnetic properties of new substituted aluminum borates $Ho_{1-x}Nd_xAl_3(BO_3)_4$ and their comparison with the properties of $HoAl_3(BO_3)_4$.

EXPERIMENT

Single crystals of $Ho_{1-x}Nd_xAl_3(BO_3)_4$ were grown from solution−melts on the basis of bismuth trimolybdate and lithium molybdate [14, 15]. The solution−melt system is conveniently presented in the quasibinary form: $(100 - n)$ wt % $[Bi_2Mo_3O_{12} + 1.5B_2O_3 + 0.4Li_2MoO_4] + n$ wt % $Ho_{1-x}Nd_xAl_3(BO_3)_4$. For $x = 0.2$ and 0.5, the concentration of crystal-forming oxides corresponding to the stoichiometry is $n = 10$

and 9%, respectively. Unfortunately, $NdAl_3(BO_3)_4$ is outside the limit of the stability of the trigonal phase. Therefore, $Y_{0.65}Nd_{0.35}Al_3(BO_3)_4$ crystals were grown.

Magnetic properties were studied using a PPMS-9 (Quantum Design) in the temperature range of 2–300 K and magnetic fields up to 9 T. Magnetoelectric studies were performed by measuring the charge between two contacts applied to opposite sides of a plane-parallel plate using a Keithley 6517B electrometer.

COMPUTATIONAL TECHNIQUE

In our calculations, we used the results of studying compounds isostructural to $Ho_{1-x}Nd_xAl_3(BO_3)_4$: $HoAl_3(BO_3)_4$ [11, 16], $TmAl_3(BO_3)_4$ [17], $HoGa_3(BO_3)_4$ [5], iron borates $HoFe_3(BO_3)_4$ [18] and with other R [2, 19], as well as paramagnetic zircons RXO_4 (X = P, V) [20].

For calculating the magnetic characteristics and the Zeeman effect, we used Hamiltonian $\mathcal{H}$ including the crystal field Hamiltonian $\mathcal{H}_{cf}$, Zeeman term $\mathcal{H}_Z$, and magnetoelastic Hamiltonian $\mathcal{H}_{me}$ written in the multipole approximation:

$$\mathcal{H} = \mathcal{H}_{cf} + \mathcal{H}_Z + \mathcal{H}_{me}, \qquad (1)$$

where

$$\mathcal{H}_{cf} = B_0^2 C_0^{(2)} + B_0^4 C_0^{(4)} + i B_{-3}^4 (C_{-3}^{(4)} + C_3^{(4)})$$
$$+ B_0^6 C_0^{(6)} + i B_{-3}^6 (C_{-3}^{(6)} + C_3^{(6)}) + B_6^6 (C_{-6}^{(6)} + C_6^{(6)}), \qquad (2)$$

$$\mathcal{H}_Z = -g_J \mu_B \mathbf{B} \mathbf{J}. \qquad (3)$$

Here, B_q^k are the crystal field parameters for the D_3 symmetry, C_q^k are irreducible tensor operators, g_J is the Landé factor, and $\mathbf{J}$ is the angular momentum operator for the R ion. The magnetoelastic Hamiltonian $\mathcal{H}_{me}$ of the R subsystem for a crystal of trigonal symmetry taking into account fourth-order operators was written earlier in [19].

The holmium and neodymium subsystems contribute to the magnetization of paramagnetic compounds $Ho_{1-x}Nd_xAl_3(BO_3)_4$ in the external field $\mathbf{B}$:

$$M = (1-x)m^{Ho} + xm^{Nd}, \quad \mathbf{m}^R = g_J^R \mu_B \langle \mathbf{J}^R \rangle. \quad (4)$$

RESULTS AND DISCUSSION

The description of the magnetic properties of $Ho_{1-x}Nd_xAl_3(BO_3)_4$ should be started from the determination of the crystal field parameters B_q^k, since namely the crystal field forming the electron structure of the R ion (its spectrum and wavefunctions) is responsible for the anisotropy of magnetic properties.

The crystal field parameters for the Ho^{3+} ion in $HoAl_3(BO_3)_4$ were determined in [11, 16],[1] where the experimental data for the temperature and field dependences of the magnetization and magnetostriction were interpreted. Since these crystal field parameters made it possible to describe well all measured magnetic and magnetoelastic properties of $HoAl_3(BO_3)_4$, they were used as the initial parameters for $Ho_{1-x}Nd_xAl_3(BO_3)_4$, from which the minimization procedure of the corresponding target function started. The parameters for $YAl_3(BO_3)_4$:Ho^{3+} [21], $NdAl_3(BO_3)_4$ [22], $TmAl_3(BO_3)_4$ [17], and $HoFe_3(BO_3)_4$ [18] were also used when searching for the crystal field parameters.

To determine the crystal field parameters, data about the magnetization curves $M_{c,\perp c}(B)$ at $T = 3$ K in fields up to 9 T and temperature dependences of the magnetization $M_{c,\perp c}(T)$ from 3 to 300 K at $B = 0.1$ and 9 T were input to the target function. On the basis of the criteria of the description of $M_{c,\perp c}(T, B)$ and the closeness of the structure of the ground multiplet to that found in $YAl_3(BO_3)_4$:Ho^{3+} [21] and $NdAl_3(BO_3)_4$ [22], we chose a set that makes it possible to describe best the entire body of experimental data ($B_q^k = (x = 0.2[x = 0.5])$, in cm^{-1}):

$$B_0^2 = 566[413], \quad B_0^4 = -1470[-1338],$$
$$B_{-3}^4 = -260[-248], \quad B_0^6 = 37[10], \qquad (5)$$
$$B_{-3}^6 = -390[-462], \quad B_6^6 = -527[-477].$$

Since these parameters were determined in the calculations in the ground multiplet basis, they can be considered only as applicable for the description of the thermodynamic properties of $Ho_{1-x}Nd_xAl_3(BO_3)_4$.

As can be seen from the magnetization curves $M_{c,\perp c}(B)$ of $Ho_{1-x}Nd_xAl_3(BO_3)_4$ ($x = 0.2, 0.5$) at $T = 3$ K given in Fig. 1, the dependences $M_{c,\perp c}(B)$ for different compounds increase with the field at different rates, demonstrating a noticeable anisotropy, which decreases with an increase in the parameter x. The dependences $M_{c,\perp c}(B)$ calculated for each compound describe well the experimental curves. The comparison of $M_{c,\perp c}(B)$ for $Ho_{1-x}Nd_xAl_3(BO_3)_4$ and $HoAl_3(BO_3)_4$ (see Fig. 1 in [11]) shows that the substitution of Nd^{3+} for Ho^{3+} leads to a slight decrease in the magnetic anisotropy. The character of the dependences $M_{c,\perp c}(B)$ is similar to that found in $HoAl_3(BO_3)_4$, since the contribution from the Ho subsystem dominates. In the field $B = 9$ T, the contribution of the Ho subsystem is ~97% in M_c and ~95% in

---

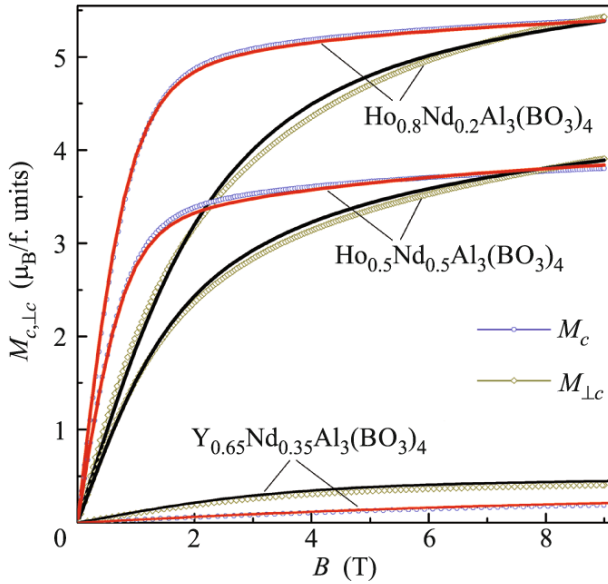[1] The parameter B_6^6 in the Russian version of [16] should be -671 cm^{-1}.

Fig. 1. (Color online) Magnetization curves of $Ho_{1-x}Nd_xAl_3(BO_3)_4$ ($x = 0.2$, 0.5) and $Y_{0.65}Nd_{0.35}Al_3(BO_3)_4$ for $\mathbf{B} \parallel \mathbf{c}$ and $\mathbf{B} \perp \mathbf{c}$ at $T = 3$ K: experimental points in comparison with calculated lines.
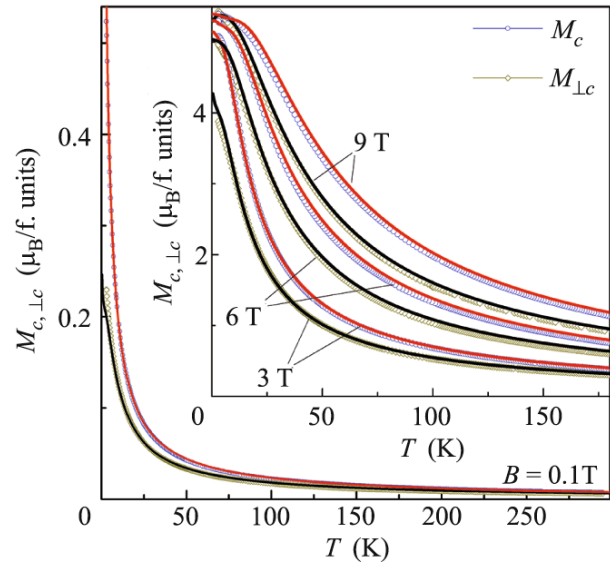

Fig. 2. (Color online) Temperature dependences of the magnetization curves $M_{c, \perp c}(T)$ of $Ho_{0.8}Nd_{0.2}Al_3(BO_3)_4$ at $B = 0.1$ T. The inset shows the dependences $M_{c, \perp c}(T)$ at $B = 3$, 6, and 9 T. Experimental points in comparison with calculated lines (red for $M_c(T)$ and black for $M_{\perp c}(T)$).

$M_{\perp c}$ for the compound with $x = 0.2$ and ~89% in M_c and ~82% in $M_{\perp c}$ for $x = 0.5$.

To understand the features of the contribution of the Nd subsystem to the magnetic properties of $Ho_{1-x}Nd_xAl_3(BO_3)_4$, we measured the dependences $M_{c, \perp c}(B)$ for $Y_{0.65}Nd_{0.35}Al_3(BO_3)_4$, which are also given in Fig. 1. It can be seen that the easy magnetization direction in $Y_{0.65}Nd_{0.35}Al_3(BO_3)_4$, in contrast to $Ho_{1-x}Nd_xAl_3(BO_3)_4$ ($x = 0$ [11], 0.2, 0.5), is the direction of the magnetic field in the basis plane ($M_{\perp c} > M_c$). Therefore, the substitution of Nd^{3+} for Ho^{3+} leads to a slight decrease in the magnetic anisotropy in $Ho_{1-x}Nd_xAl_3(BO_3)_4$. The calculation of the curves $M_{c, \perp c}(B)$ for $Y_{0.65}Nd_{0.35}Al_3(BO_3)_4$ showed that the crystal field parameters for pure $NdAl_3(BO_3)_4$ from [22] make it possible to describe the experiment satisfactorily.

The temperature dependences of the magnetization $M_{c, \perp c}(T)$ of $Ho_{0.8}Nd_{0.2}Al_3(BO_3)_4$ in the field $B = 0.1$ T shown in Fig. 2 and (inset) in high fields $B = 3$, 6, and 9 T indicate that the anisotropy of the curves $M_{c, \perp c}(T)$ at low T values decreases with the increase in B and is described well in the whole temperature range. A similar good description of $M_{c, \perp c}(T)$ at $B = 0.1$, 3, 6, and 9 T was also achieved for the compound with $x = 0.5$. The analysis of the $M_c/M_{\perp c}$ values shows that the anisotropy decreases for $B = 0.1$ and 3 T and increases slightly for $B = 6$ and 9 T in comparison with $HoAl_3(BO_3)_4$. For example, for $Ho_{0.8}Nd_{0.2}Al_3(BO_3)_4$ ($HoAl_3(BO_3)_4$) at $T = 5$ K, $M_c/M_{\perp c} = 1.99$ (2.21), 1.34

(1.35), 1.08 (1.07), and 1.00 (0.99) for $B = 0.1$, 3, 6, and 9 T, respectively.

The dependences $M_c - M_{\perp c}(T)$ for (open symbols) $Ho_{0.8}Nd_{0.2}Al_3(BO_3)_4$ and (closed symbols) $HoAl_3(BO_3)_4$ at $B = 0.1-9$ T shown in Fig. 3 make it possible to analyze the dependence of the magnetic
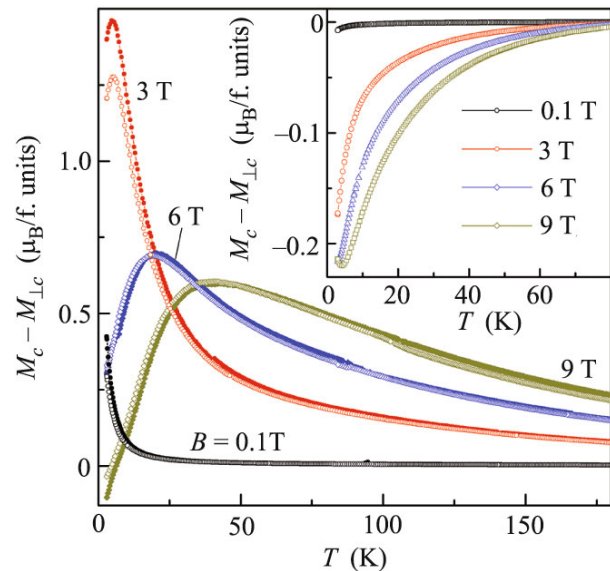

Fig. 3. (Color online) Experimental temperature dependences of $M_c - M_{\perp c}(T)$ for (open symbols) $Ho_{0.8}Nd_{0.2}Al_3(BO_3)_4$ and (closed symbols) $HoAl_3(BO_3)_4$ at $B = 0.1$, 3, 6, and 9 T. The inset shows the low-temperature region of $M_c - M_{\perp c}(T)$ for $Y_{0.65}Nd_{0.35}Al_3(BO_3)_4$.

anisotropy on T and B. It can be seen that the curves $M_c - M_{\perp c}(T)$ for $Ho_{0.8}Nd_{0.2}Al_3(BO_3)_4$ at $B = 0.1$ and 3 T are lower (the anisotropy is less) than the curves for $HoAl_3(BO_3)_4$. For the higher field $B = 9$ T (and partially for 6 T), on the contrary, the curves $M_c - M_{\perp c}(T)$ for $Ho_{0.8}Nd_{0.2}Al_3(BO_3)_4$ lie higher, but this relation changes with an increase in T, and the anisotropy again becomes less than that in $HoAl_3(BO_3)_4$. The analysis of the dependences $M_c - M_{\perp c}(T)$ for $Y_{0.65}Nd_{0.35}Al_3(BO_3)_4$ (inset in Fig. 3) shows that the contribution of the Nd subsystem to the magnetic anisotropy of $Ho_{1-x}Nd_xAl_3(BO_3)_4$ has the other sign and is significant for $T < 60$ K and $B > 0.1$ T.

We consider the contribution of the Ho subsystem to the magnetic anisotropy of $Ho_{1-x}Nd_xAl_3(BO_3)_4$. Since the curves $M_c - M_{\perp c}(T) < 0$ for $Y_{0.65}Nd_{0.35}Al_3(BO_3)_4$ (see inset in Fig. 3) and the resultant curves $M_c - M_{\perp c}(T)$ for $Ho_{0.8}Nd_{0.2}Al_3(BO_3)_4$ except for the low-temperature region for $B = 3$ T are close to the curves for $HoAl_3(BO_3)_4$, the contribution of the Ho subsystem to the magnetic anisotropy of $Ho_{1-x}Nd_xAl_3(BO_3)_4$ is much more anisotropic than that in $HoAl_3(BO_3)_4$. The estimate of the values $M_c - M_{\perp c}(T)$ for $Ho_{0.8}Nd_{0.2}Al_3(BO_3)_4$ minus values for $Y_{0.65}Nd_{0.35}Al_3(BO_3)_4$, i.e., the contribution from the Ho subsystem, shows that the anisotropy in the Ho subsystem with respect to $HoAl_3(BO_3)_4$ at $T = 5$ K hardly changed in a field of 3 T and increased by a factor of ~1.5 and 7 in a field of 6 and 9 T, respectively.

It is clear from the above that $Ho_{1-x}Nd_xAl_3(BO_3)_4$ ($x = 0.2, 0.5$) and $HoAl_3(BO_3)_4$ demonstrate close magnetic properties. One observes a slight decrease in the resultant magnetic anisotropy with the increase in the parameter x. We consider how the record-high polarization of $HoAl_3(BO_3)_4$ was affected by the substitution of Nd^{3+} for Ho^{3+}, varied crystal field, and magnetic anisotropy.

The subsequent figures show the field dependences of the longitudinal ($\Delta P_{aa}(B_a)$) and transverse ($\Delta P_{ab}(B_b)$) polarization of $Ho_{0.8}Nd_{0.2}Al_3(BO_3)_4$ (Fig. 4) and $Ho_{0.5}Nd_{0.5}Al_3(BO_3)_4$ (Fig. 5). As in $HoAl_3(BO_3)_4$, an increase in the field is accompanied by a similar strong increase in the anisotropic curves $\Delta P_a(B_{a,b})$.[2] The observed polarization reaches at $T = 5$ K in 9 T the value $\Delta P_{ab}(B_b) \approx -2630$ and -1380 $\mu C/m^2$ for $Ho_{0.8}Nd_{0.2}Al_3(BO_3)_4$ and $Ho_{0.5}Nd_{0.5}Al_3(BO_3)_4$, respectively. These ΔP values strongly exceed all known values (given below in $\mu C/m^2$) for iron borates (~300 in $NdFe_3(BO_3)_4$ [23] and $HoFe_3(BO_3)_4$ [24], ~500 in $SmFe_3(BO_3)_4$ [25], ~900 in $Ho_{0.5}Nd_{0.5}Fe_3(BO_3)_4$ [13], and ~1000 in $Ho_{0.75}Nd_{0.25}Fe_3(BO_3)_4$ [26]), aluminum borates (~140

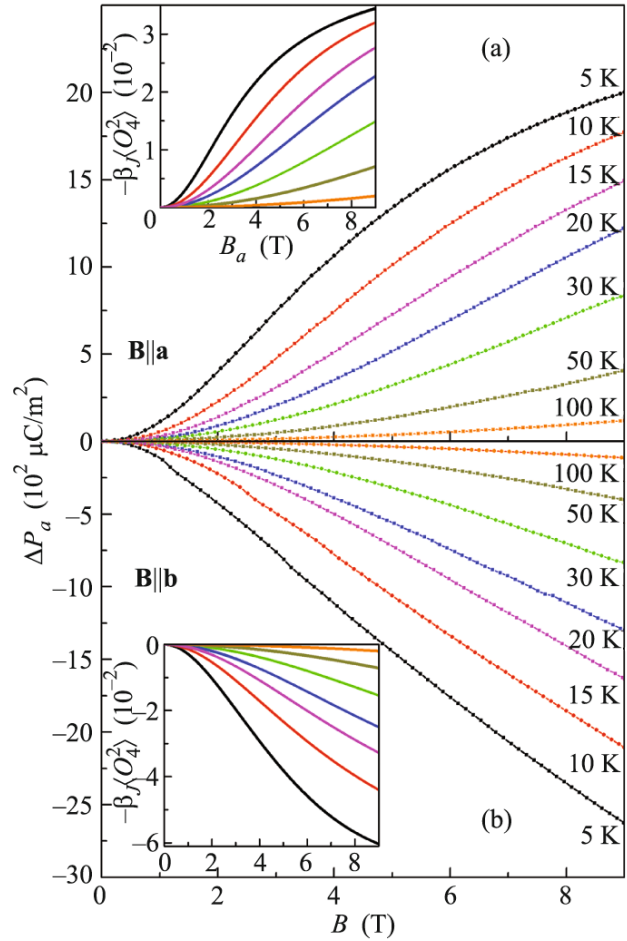**Fig. 4.** (Color online) Experimental field dependences of the (a) longitudinal and (b) transverse magnetoelectric polarization of $Ho_{0.8}Nd_{0.2}Al_3(BO_3)_4$ at the indicated temperatures. The insets show the field dependences of the multipole moment $-\beta_J \langle O_4^2 \rangle$ for (a) $\mathbf{B} \parallel \mathbf{a}$ and (b) $\mathbf{B} \parallel \mathbf{b}$ (curves for the corresponding temperatures are shown in the same colors).

---

in $ErAl_3(BO_3)_4$ [10] and ~750 in $TmAl_3(BO_3)_4$ [8, 10]), and galloborate $HoGa_3(BO_3)_4$ (~1020) [5], and they are the second best result, yielding only to the record-high value in $HoAl_3(BO_3)_4$ (~5240) [11]. The measurements indicated that the polarization for $\mathbf{B} \parallel \mathbf{c}$ is much less than that at $\mathbf{B} \perp \mathbf{c}$ as in $HoAl_3(BO_3)_4$.

Thus, it was established that the expected high magnetoelectric effect is implemented in $Ho_{1-x}Nd_xAl_3(BO_3)_4$. However, the expected enhancement of the effect did not take place. We checked the possibility of the effect of the inverse twinning in $Ho_{1-x}Nd_xAl_3(BO_3)_4$ single crystals on the result obtained. The X-ray studies of the twinning factor showed that $Ho_{0.8}Nd_{0.2}Al_3(BO_3)_4$ and $Ho_{0.5}Nd_{0.5}Al_3(BO_3)_4$ are left-handed by 100 and 81%, respectively.

---

[2] In [11], the subscript b in ΔP and B should be replaced by a and vice versa. For example, it should be $\Delta P_{ab}(B_b)$ instead of $\Delta P_{ba}(B_a)$.

Fig. 5. (Color online) Experimental field dependences of the (a) longitudinal and (b) transverse magnetoelectric polarization of $Ho_{0.5}Nd_{0.5}Al_3(BO_3)_4$ at the indicated temperatures. The insets show the field dependences of the multipole moment $-\beta_J\langle O_4^2\rangle$ for (a) $\mathbf{B}\parallel\mathbf{a}$ and (b) $\mathbf{B}\parallel\mathbf{b}$ (curves for the corresponding temperatures are shown in the same colors).
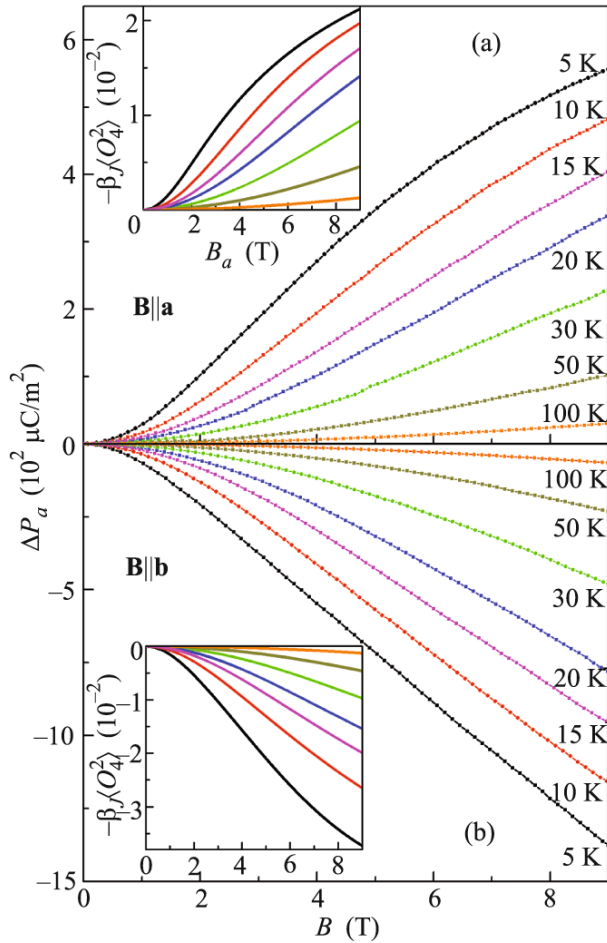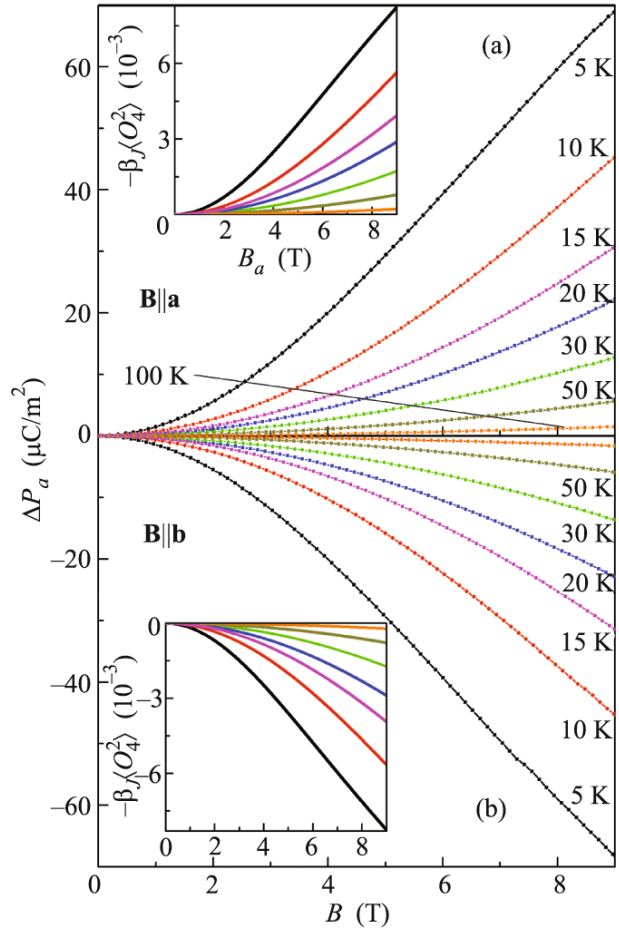

Fig. 6. (Color online) Experimental field dependences of the (a) longitudinal and (b) transverse magnetoelectric polarization of $Y_{0.65}Nd_{0.35}Al_3(BO_3)_4$ at the indicated temperatures. The insets show the field dependences of the multipole moment $-\beta_J\langle O_4^2\rangle$ for (a) $\mathbf{B}\parallel\mathbf{a}$ and (b) $\mathbf{B}\parallel\mathbf{b}$ (curves for the corresponding temperatures are shown in the same colors).

To understand the features of the contribution of the Nd subsystem to the magnetoelectric properties of $Ho_{1-x}Nd_xAl_3(BO_3)_4$, we measured the field dependences $\Delta P_a(B_{abc})$ for the $Y_{0.65}Nd_{0.35}Al_3(BO_3)_4$ crystal. It is clear from Fig. 6 that $Y_{0.65}Nd_{0.35}Al_3(BO_3)_4$ does not demonstrate high ΔP values possible in analogy with iron borate $NdFe_3(BO_3)_4$. At $T = 5$ K in the field $B = 9$ T, $\Delta P_{ab}(B_b)$ and $\Delta P_{aa}(B_a) \approx 70$ μC/m² and $\Delta P_{ac}(B_c) \approx 1$ μC/m².

With allowance for the small contribution to the polarization from the Nd subsystem, it is possible to assume that the main origin of the observed decrease in ΔP in $Ho_{1-x}Nd_xAl_3(BO_3)_4$ (in comparison with $HoAl_3(BO_3)_4$) is associated with the decreased contribution from the Ho_{1-x} subsystem. However, the study of $HoGa_3(BO_3)_4$ [5] showed a much stronger decrease

in ΔP (by a factor of ~5) in comparison with $HoAl_3(BO_3)_4$. The polarization in $Ho_{0.8}Nd_{0.2}Al_3(BO_3)_4$ and in half-substituted $Ho_{0.5}Nd_{0.5}Al_3(BO_3)_4$ decreased by a factor of ~2 and 3.8, respectively. We note that, if the resultant polarization was the sum of contributions from the values in the pure compounds, the $\Delta P_{ab}(B_b)$ value in $Ho_{0.8}Nd_{0.2}Al_3(BO_3)_4$ would be ~1.6 times higher (~4262 μC/m²) than that found. Interestingly, the revealed slight decrease in the magnetic anisotropy in $Ho_{1-x}Nd_xAl_3(BO_3)_4$ (in comparison with $HoAl_3(BO_3)_4$), which, according to [9, 10], should increase ΔP, does not produce a noticeable effect.

Since the contribution to the polarization from the Nd subsystem is small, it is possible to assume that the main origin of the decrease in ΔP is a qualitative change in the contribution from the Ho_{1-x} subsystem,

rather than its decrease. As was noted above when analyzing Fig. 3, the contribution of the Ho subsystem to the magnetic anisotropy of $Ho_{0.8}Nd_{0.2}Al_3(BO_3)_4$ at $B > 3$ T became more anisotropic than that in $HoAl_3(BO_3)_4$. According to [9, 10], this leads to the decrease in the contribution from the Ho subsystem to the total polarization of the system. The increase in the magnetic anisotropy in the Ho subsystem in $Ho_{1-x}Nd_xAl_3(BO_3)_4$ is associated with the changed crystal field (owing to the substitution of Nd^{3+} for Ho^{3+}), which forms the electron structure of the Ho^{3+} ion and is responsible for the magnetic anisotropy. The decrease in ΔP in $Ho_{0.5}Nd_{0.5}Al_3(BO_3)_4$ is also due to the observed twinning.

It was established in a number of works that there are stable correlations between the magnetoelectric and magnetoelastic properties of borates $RM_3(BO_3)_4$. For example, the correlation between the field dependences of the polarization and magnetostriction was found in $TmAl_3(BO_3)_4$ [8], $HoAl_3(BO_3)_4$ [9], iron borates [7, 24], and $Ho_{0.75}Nd_{0.25}Fe_3(BO_3)_4$ [26]. Recently, it was shown that the difference in the ΔP values in $HoFe_3(BO_3)_4$ and $HoAl_3(BO_3)_4$ is mainly due to the difference in the magnetostriction values [12]. The authors of [12] believe that the magnetoelectric effect arising in $RM_3(BO_3)_4$ is determined by the magnetostriction and piezoelectricity. Lattice deformation that determines the appearance of the polarization occurs in the magnetic field. It is possible to assume that the crystal field in $Ho_{1-x}Nd_xAl_3(BO_3)_4$ that changed owing to the substitution determines the increase in the magnetic anisotropy in the Ho subsystem, which leads to a lower value of magnetostriction and, as a consequence, polarization.

Magnetoelastic phenomena (magnetostriction, anomalies of the lattice parameters and elastic constants) depend strongly on the R ion and its electron structure (formed by the crystal field) and are due to the variation of the asphericity of the $4f$ shell of the R ion under the variation of the external parameters (magnetic field, temperature, etc.). Multipole moments are an adequate characteristic of the asphericity of the $4f$ shell of the R ion. The calculated field and temperature dependences of the multipole moments in $HoAl_3(BO_3)_4$ [16] and $TmAl_3(BO_3)_4$ [17] made it possible to describe the magnetostriction found in them. Such calculations were also performed for iron borates (see, e.g., [19]). With allowance for the established correlation of the magnetoelectric and magnetoelastic properties, we performed calculations for $Ho_{1-x}Nd_xAl_3(BO_3)_4$ analogous to those in [16, 17, 5] and compared their results with the dependences $\Delta P(B)$ (the magnetoelastic Hamiltonian and the expression for the magnetostriction see in [19] and [16, 17], respectively).

According to [16, 17, 5], the largest moments $-\beta_J \langle O_4^2 \rangle$ and $-\alpha_J \langle O_2^2 \rangle$ are responsible for the behavior

of the magnetostriction at $\mathbf{B} \perp \mathbf{c}$. Insets in Figs. 4 and 5 show the field dependences of the moment $-\beta_J \langle O_4^2 \rangle$ most strongly varying with the field calculated with the crystal field parameters given in Eqs. (5) and with the inclusion of the contributions from the Ho and Nd subsystems ($\beta_J \langle O_4^2 \rangle = (1-x)\beta_J^{Ho} \langle O_4^2 \rangle^{Ho} + x\beta_J^{Nd} \langle O_4^2 \rangle^{Nd}$) at the temperatures at which $\Delta P_a(B_{a,b})$ were measured. It can be seen that the character of the field and temperature dependences of the moment $-\beta_J \langle O_4^2 \rangle$ is in complete qualitative agreement with dependences $\Delta P_a(B_{a,b}, T)$ and predicts a similar nonlinear form of the unstudied experimental magnetostriction. Dependences $-\alpha_J \langle O_2^2 \rangle$ $(B_{a,b}, T)$ of the second actual moment are close to the shown quantities $-\beta_J \langle O_4^2 \rangle$ $(B_{a,b}, T)$. We note that the moments $-\beta_J \langle O_4^2 \rangle$ and $-\alpha_J \langle O_2^2 \rangle$, as well as ΔP_a, have opposite signs at $\mathbf{B} \| \mathbf{a}$ and $\mathbf{B} \| \mathbf{b}$. Accordingly, opposite signs of the magnetostriction are expected for these field directions as well. In addition, at $\mathbf{B} \| \mathbf{b}$, the actual moments vary with the field more strongly than at $\mathbf{B} \| \mathbf{a}$. Consequently, the magnetostriction $\Delta a/a$ at $\mathbf{B} \| \mathbf{b}$ should be larger than that at $\mathbf{B} \| \mathbf{a}$, which correlates with the relations of polarizations at $\mathbf{B} \| \mathbf{a}, \mathbf{b}$ and results [9].

Figure 6 shows dependences $\beta_J^{Nd} \langle O_4^2 \rangle^{Nd}(B_{a,b}, T)$ for $Y_{0.65}Nd_{0.35}Al_3(BO_3)_4$ calculated with the crystal field parameters for $NdAl_3(BO_3)_4$ from [22], which are described well by curves $\Delta P_a(B_{a,b}, T)$. It can be seen that the values $\beta_J^{Nd} \langle O_4^2 \rangle^{Nd}$ at $\mathbf{B} \| \mathbf{a}$ and $\mathbf{B} \| \mathbf{b}$ are close to each other, which corresponds to close values ΔP_a for these field directions.

Since the used theoretical approach makes it possible to describe well the main features of the curves $\Delta P_a(B)$ at $B_{a,b} < 9$ T, it is of interest to perform calculations for high magnetic fields, in which no measurements have been performed yet, and, thus, to predict the further behavior of the polarization, in particular, the possibility of the continuation of the growth or the presence of saturation. We performed such calculations for $Ho_{1-x}Nd_xAl_3(BO_3)_4$ ($x = 0.2, 0.5$) and $HoAl_3(BO_3)_4$. As supposed, the results were close. At $\mathbf{B} \perp \mathbf{c}$ in fields up to 25 T, the moments $-\alpha_J \langle O_2^2 \rangle$ and $-\beta_J \langle O_4^2 \rangle$ change the most. For fields $B_{\perp c} < 9$ T, these moments are close to each other, whereas above 10 T, the moment $-\beta_J \langle O_4^2 \rangle$ demonstrates a broad peak and decreases, and $-\alpha_J \langle O_2^2 \rangle$ continues to increase gradually. Thus, it is possible to assume that the magnetostriction and polarization curves in fields $B_{\perp c} > 9$ T will change the sharp increase to a gradual increase up to 14 T (by 5−7%) and, then, either a broad peak and the decrease in $\Delta P(B)$) or the continuation of the smooth

increase will be observed depending on the moment making the largest contribution.

CONCLUSIONS

In summary, we have studied the thermodynamic properties of $Ho_{1-x}Nd_xAl_3(BO_3)_4$ and $Y_{0.65}Nd_{0.35}Al_3(BO_3)_4$. It has been established that $Ho_{1-x}Nd_xAl_3(BO_3)_4$ ($x = 0.2, 0.5$) exhibits a strong magnetoelectric effect yielding only to that in $HoAl_3(BO_3)_4$ among borates $RM_3(BO_3)_4$. The comparison with the properties of $HoAl_3(BO_3)_4$ demonstrating record-high polarization values has allowed analyzing the possible origins of the decrease in the polarization in $Ho_{1-x}Nd_xAl_3(BO_3)_4$ and indicating the strong effect of the crystal field on the magnetoelectric properties. The determined parameters have made it possible to interpret all measured properties and found features within the unified approach.

The possible experimental study of the polarization and magnetostriction of $HoAl_3(BO_3)_4$ and $Ho_{1-x}Nd_xAl_3(BO_3)_4$ in fields $B_{\perp c} > 9$ T will make it possible to check the predictions of their behavior and thus to establish the main moments. Further, this should help in the description and prediction of the possible colossal ΔP values in the borates $RM_3(BO_3)_4$ not studied yet.

REFERENCES

1. A. K. Zvezdin, S. S. Krotov, A. M. Kadomtseva, G. P. Vorob'ev, A. P. Pyatakov, L. N. Bezmaternykh, and E. A. Popova, JETP Lett. **81**, 272 (2005).

2. E. A. Popova, D. V. Volkov, A. N. Vasiliev, A. A. Demidov, N. P. Kolmakova, I. A. Gudim, L. N. Bezmaternykh, N. Tristan, Yu. Skourski, B. Buechner, C. Hess, and R. Klingeler, Phys. Rev. B **75**, 224413 (2007).

3. A. I. Popov, D. I. Plokhov, and A. K. Zvezdin, Phys. Rev. B **87**, 024413 (2013).

4. T. Usui, Y. Tanaka, H. Nakajima, M. Taguchi, A. Chainani, M. Oura, S. Shin, N. Katayama, H. Sawa, Y. Wakabayashi, and T. Kimura, Nature Mater. **13**, 611 (2014).

5. N. V. Volkov, I. A. Gudim, E. V. Eremin, A. I. Begunov, A. A. Demidov, and K. N. Boldyrev, JETP Lett. **99**, 67 (2014).

6. A. M. Kadomtseva, Yu. F. Popov, G. P. Vorob'ev, N. V. Kostyuchenko, A. I. Popov, A. A. Mukhin, V. Yu. Ivanov, L. N. Bezmaternykh, I. A. Gudim, V. L. Temerov, A. P. Pyatakov, and A. K. Zvezdin, Phys. Rev. B **89**, 014418 (2014).

7. A. M. Kadomtseva, Yu. F. Popov, G. P. Vorob'ev, A. P. Pyatakov, S. S. Krotov, K. I. Kamilov, V. Yu. Ivanov, A. A. Mukhin, A. K. Zvezdin, A. M. Kuz'menko, L. N. Bezmaternykh, I. A. Gudim, and V. L. Temerov, Low Temp. Phys. **36**, 511 (2010).

8. R. P. Chaudhury, B. Lorenz, Y. Y. Sun, L. N. Bezmaternykh, V. L. Temerov, and C. W. Chu, Phys. Rev. B **81**, 220402 (2010).

9. K.-C. Liang, R. P. Chaudhury, B. Lorenz, Y. Y. Sun, L. N. Bezmaternykh, V. L. Temerov, and C. W. Chu, Phys. Rev. B **83**, 180417(R) (2011).

10. K.-C. Liang, R. P. Chaudhury, B. Lorenz, Y. Y. Sun, L. N. Bezmaternykh, I. A. Gudim, V. L. Temerov, and C. W. Chu, J. Phys.: Conf. Ser. **400**, 032046 (2012).

11. A. I. Begunov, A. A. Demidov, I. A. Gudim, and E. V. Eremin, JETP Lett. **97**, 528 (2013).

12. V. I. Zinenko, M. S. Pavlovskii, A. S. Krylov, I. A. Gudim, and E. V. Eremin, J. Exp. Theor. Phys. **117**, 1032 (2013).

13. R. P. Chaudhury, F. Yen, B. Lorenz, Y. Y. Sun, L. N. Bezmaternykh, V. L. Temerov, and C. W. Chu, Phys. Rev. B **80**, 104424 (2009).

14. L. N. Bezmaternykh, V. L. Temerov, I. A. Gudim, and N. A. Stolbovaya, Crystallogr. Rep. **50**, 97 (2005).

15. V. L. Temerov, A. E. Sokolov, A. L. Sukhachev, A. F. Bovina, I. S. Edelman, and A. V. Malakhovskii, Crystallogr. Rep. **53**, 1157 (2008).

16. A. I. Begunov, D. V. Volkov, and A. A. Demidov, Phys. Solid State **56**, 511 (2014).

17. A. A. Demidov, D. V. Volkov, I. A. Gudim, E. V. Eremin, and K. N. Boldyrev, J. Exp. Theor. Phys. **119**, 737 (2014).

18. A. A. Demidov and D. V. Volkov, Phys. Solid State **53**, 985 (2011).

19. A. A. Demidov, N. P. Kolmakova, L. V. Takunov, and D. V. Volkov, Physica B **398**, 78 (2007).

20. A. A. Demidov, Z. A. Kazei, N. P. Kolmakova, J.-M. Broto, and H. Racoto, Phys. Rev. B **70**, 134432 (2004).

21. A. Baraldi, R. Capelletti, M. Mazzera, N. Magnani, I. Foldvari, and E. Beregi, Phys. Rev. B **76**, 165130 (2007).

22. C. Cascales, C. Zaldo, U. Caldino, J. Garcia Sole, and Z. D. Luo, J. Phys.: Condens. Matter **13**, 8071 (2001).

23. A. K. Zvezdin, G. P. Vorob'ev, A. M. Kadomtseva, Yu. F. Popov, A. P. Pyatakov, L. N. Bezmaternykh, A. V. Kuvardin, and E. A. Popova, JETP Lett. **83**, 509 (2006).

24. A. M. Kadomtseva, G. P. Vorob'ev, Yu. F. Popov, A. P. Pyatakov, A. A. Mukhin, V. Yu. Ivanov, A. K. Zvezdin, I. A. Gudim, V. L. Temerov, and L. N. Bezmaternykh, J. Exp. Theor. Phys. **114**, 810 (2012).

25. Yu. F. Popov, A. P. Pyatakov, A. M. Kadomtseva, G. P. Vorob'ev, A. K. Zvezdin, A. A. Mukhin, V. Yu. Ivanov, and I. A. Gudim, J. Exp. Theor. Phys. **111**, 199 (2010).

26. G. P. Vorob'ev, Yu. F. Popov, A. M. Kadomtseva, E. V. Kuvardin, A. A. Mukhin, V. Yu. Ivanov, L. N. Bezmaternykh, I. A. Gudim, and V. L. Temerov, in *Proceedings of the 3rd International Interdisciplinar Symposium on Media with Structural and Magnetic Ordering (Multiferroics-3), Rostov-on-Don, 2011*.

Translated by L. Mosina